Cancer Nanotechnology

RESEARCH Open Access

Fabrication and application of cisplatin-loaded mesoporous magnetic nanobiocomposite: a novel approach to smart cervical cancer chemotherapy

Mahdieh Darroudi[1,2†], Seyedeh Elnaz Nazari[1†], Fereshteh Asgharzadeh[1], Nima Khalili-Tanha[1], Ghazaleh Khalili-Tanha[3,4], Toktam Dehghani[5], Maryam Karimzadeh[2], Mina Maftooh[4], Gordon A. Fern[6], Amir Avan[3,4], Majid Rezayi[2,4,7*] and Majid Khazaei[1,4*]

†Mahdieh Darroudi and Seyedeh Elnaz Nazari have equal contribution and are co-first authors

*Correspondence: rezaeimj@mums.ac.ir; khazaeim@mums.ac.ir

[1] Metabolic Syndrome Research center, Department of Physiology, Faculty of Medicine, Mashhad University of Medical Science, Mashhad, Iran
[2] Department of Medical Biotechnology and Nanotechnology, School of Science, Mashhad University of Medical Science, Mashhad, Iran
Full list of author information is available at the end of the article

Abstract

There are significant challenges in developing drug carriers for therapeutic perspective. We have investigated a novel nanocarrier system, based on combining functionalized magnetic nanocomposite with Metal–Organic Frameworks (MOFs). Magnetic nanoparticles modified using biocompatible copolymers may be suitable for delivering hydrophobic drugs, such as cisplatin. Furthermore, compared to polymeric nanocarriers, nanocomposite constructed from zeolitic imidazolate framework-8 (ZIF-8) have demonstrated better drug loading capacity, as well as excellent pH-triggered drug release. Cisplatin-encapsulated Fe_3O_4@SiO_2-ZIF-8@N-Chit-FA has been evaluated to determine the antitumor effects of free cisplatin enhancement in cervical cancer cells. In order to increase the stability of the proposed nanocarrier in aqueous solutions, in addition to the density of functional groups, a nano-chitosan layer was coated on top of the magnetic nanocomposite. It was then added with cisplatin onto the surface of Fe_3O_4@SiO_2-ZIF-8@N-Chit-FA to deliver anticancer treatment that could be targeted using a magnetic field. A mouse isograft model of TC1 cells was used to evaluate the in vivo tumor growth inhibition. In tumor-bearing mice, Fe_3O_4@SiO_2-ZIF-8@N-Chit-FA-cisplatin was injected intraperitoneally, and the targeted delivery was amplified by an external magnet (10 mm by 10 mm, surface field strength 0.4 T) fixed over the tumor site. Based on in vivo results, cisplatin-Loaded Mesoporous Magnetic Nanobiocomposite inhibited the growth of cervical tumors ($P < 0.001$) through the induction of tumor necrosis ($P < 0.05$) when compared to cisplatin alone. With the application of an external magnetic field, the drug was demonstrated to be able to induce its effects on specific target areas. In summary, Fe_3O_4 @ SiO_2-ZIF-8 @ N-Chit-FA nanocomposites have the potential to be implemented in targeted nanomedicine to deliver bio-functional molecules.

Keywords: Drug delivery, Cervical cancer, Magnetic nanocomposite, In vivo

Introduction

Cervical cancer is ranked fourth among most common malignant gynecological tumors. According to the CDC, 311,000 deaths occurred from the 570,000 cases diagnosed in 2018 (Arbyn et al. 2020). Nearly half of all deaths from cervical cancer occurred in women over 58 years of age, and cervical cancer is the second most common death cause in women 20–39 years of age (LaVigne et al. 2017; Siegel et al. 2019). However, late-stage disease and cervical adenocarcinomas remain major concern to women globally and cannot be detected by cytology (Ramezani Farani et al. 2022). Although cytology is the most widely used method for detecting cervical cancer, vaccination against human papillomavirus has proven to be very effective (Adiga et al. 2021). Despite existing trials, cervical cancer remains one of the most common causes of cancer-related deaths in women, and further research is required (Paskeh et al. 2021).

Cisplatin has a central role in cancer chemotherapy; however, its systemic toxicity poses a significant obstacle (Zhao et al. 2015). Cisplatin is used as a chemotherapy agent alone or in combination with other drugs to treat various solid tumors, such as reproductive system tumors, cervical, ovarian, head and neck tumors, and melanomas (Chon et al. 2012; Luo et al. 2021; Maillard et al. 2020; Mitsudomi et al. 2010). Despite the popularity of cisplatin in the cancer treatment, it has serious side effects that include bone marrow suppression, nephrotoxicity, neurotoxicity, dose toxicity, and hearing loss (He et al. 2022; Kuang et al. 2012; Ramkumar et al. 2021). Currently, the formulation of cisplatin is promising although some draw backs, such as short aqueous half-life, ease of oxidation and hydrolysis, and light instability, are problematic. Hence, many nanotechnology approaches, which include green methodologies, microfluidics (Rabiee et al. 2021), microporous intelligent nanostructures (Rahimnejad et al. 2021a), high-gravity approaches, and combinations (Rahimnejad et al. 2021b), are being investigated to determine if they can significantly enhance the drug's effectiveness and efficiency, reduce the cost of its development, increase its eco-friendliness, and speed up the drug discovery process (Jafari et al. 2022). Medical nanotechnology applications have driven the design of novel intelligent nano-systems, which can respond physically and morphologically to the pathological environment of tumor tissues (Gonciar et al. 2019; Huang et al. 2016; Kashyap et al. 2021; Rashid and Zaid Ahmad 2018). This has prompted the exploration of novel nano-formulations in order to overcome the limitations of conventional cancer treatments by addressing disease-specific mechanisms and properties (Ulbrich et al. 2016). The use of drug carriers significantly increases targeted drug accumulation (Tan et al. 2020) in specific organs or cell types and permits controlled release (or activation) of drugs where therapeutic effect is desired, e.g., in the tumor matrix and/or in tumor cells. Furthermore, selective activation could limit toxicity, preventing or minimizing harmful side effects (Pecorino 2021).

In this scenario, researchers have been investigating the properties of magnetic nanoparticles (Abedi et al. 2019; Boyer et al. 2010), which make role due to its various applications in Magnetic Resonance Imaging (MRI) (Smith and Gambhir 2017), magnetic separation (Guo et al. 2017), drug delivery (Darroudi et al. 2021; Vangijzegem et al. 2019), and hyperthermia chemotherapy (Vamvakidis et al. 2018b, 2018a). A magnetic field can be used to manipulate superparamagnetic nanoparticles. When the magnet is removed, there is no residual magnetization, which provides colloidal stability and

dispersibility for the NPs, thereby rendering it suitable for biomedical applications (Lee et al. 2015). The biocompatibility, biodegradability, aqueous dispersibility, and magnetic properties of magnetic NPs make them good candidates for biomedical applications (Zanganeh et al. 2016). Furthermore, the development of nanobiomaterials for drug delivery functions offers new possibilities for individualized diagnosis and treatment (Cheng et al. 2018; Yang et al. 2018; Zou et al. 2018). Metal–organic framework materials (MOFs) have a range of advantageous properties, including flexible modification, tunable pore size, and controllable synthesis (Rojas et al. 2019; Wang 2017). MOFs can also offer multiple versatilities for encapsulating and loading active ingredients (Qin et al. 2019). Mesoporous nanoscale zeolitic imidazolate framework-8 (ZIF-8) is a well-known MOF versatile nanocarrier due to its biocompatibility and biodegradability upon acidic conditions (Lv et al. 2019; Zheng et al. 2016). Through functionalizing nanocarriers, pharmacokinetics and biodistribution can be modified (Mandriota et al. 2019). In addition, the use of polymers as a vehicle for drug delivery has been receiving considerable attention in recent years due to their designability, biocompatibility, and other properties (Nejadshafiee et al. 2019). Folic acid (FA) is also an ideal targeting molecule since folate receptors are frequently expressed on cancer cells and rarely found on normal cells (Zadeh Mehrizi et al. 2018); the use of folic acid is facilitated by its natural adhesive properties and functional groups, which are able to form thin, surface-adherent polymer films onto virtually all material surfaces (Azizi et al. 2021). Phase separation and ionic gelation methods were mainly implemented to prepare nano-chitosan biocomposites (Ramezani Farani et al. 2022; Vaezifar et al. 2013). Its functionalization with folic acid is considered a good substance for the delivery of molecules due to its high solubility in water, excellent biocompatibility, and biodegradability (Jermy et al. 2021, 2019). Upon further investigation, it was found that nano-chitosan functionalized by FA behaved highly dependently on the pH value of the solution (Farahnak Roudsari et al. 2021). Herein, we present a bioinspired mesoporous and magnetic nanocomposite containing Chitosan NPs-FA-functionalization (Fe_3O_4@SiO_2-ZIF-8@N-Chit-FA) as a targeted drug delivery system (Fig. 1).

Materials and methods

Materials

All chemicals were obtained from commercial supplier and, except otherwise stated, used without further purification. Toluene, sodium tripolyphosphate (TPP), Chitosan (Chit), phosphate buffer saline (PBS), sodium dodecyl sulfate (SDS), high glucose cell culture medium, and a tetrazolium-based assay were acquired from Sigma-Aldrich. PBS at pH 7 was prepared by mixing monobasic potassium phosphate (KH_2PO_4) and dibasic potassium phosphate (K_2HPO_4) in an aqueous solution. Throughout all experiments, ultrapure water was used as a water system.

Preparation of nano-chitosan

The chitosan NPs containing FA were synthesized by Roudsari et al. with some modifications (Alishahi et al. 2011; Farahnak Roudsari et al. 2021). A transparent chitosan solution was prepared by dissolving chitosan in 1% (w/v) acetic acid using a magnetic stirrer, followed by diluting with deionized water to create a solution with a final concentration

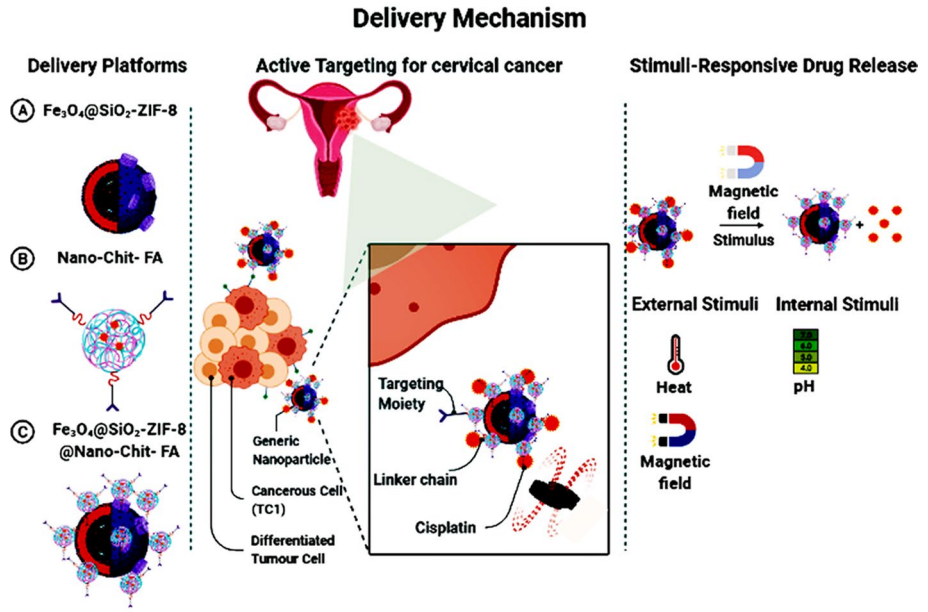

Fig. 1 **a** Fabrication of Fe_3O_4@SiO_2-ZIF-8@N-Chit-FA, **b** Schematic of in vivo targeted drug delivery of cisplatin against cervical cancer

of 0.1 (w/v) at pH 5. TPP solution at a concentration of 0.05% (w/v) was added dropwise with an equal volume of chitosan solution for 15 min to induce the spontaneous formation of chitosan–TPP nanoparticles by ionic gelation mechanism. To prepare chitosan–TPP nanoparticles coated with FA, the suspension was stirred by stirring for 60 min at room temperature, followed by crosslinking the amino groups of chitosan–TPP and FA. We isolated the nanoparticles by centrifuging the solution at 8000 rpm for 30 min and drying the precipitate in a freeze dryer.

Synthesis of Fe_3O_4@SiO_2@ZIF-8 nanoparticles

A facile solvothermal method was used to prepare the magnetic Fe_3O_4@SiO_2 core–shell (Darroudi et al. 2020; Ghasemi et al. 2021). Afterward, a solution of $Zn(NO_3)_2$.6 H_2O and 2-methyl imidazolate in methanol, 15 mg of Fe_3O_4@SiO_2 core–shell, was used for 1 h at 60 °C, stirring vigorously throughout the reaction. Following cooling to room temperature, the mixture was separated using a magnet and washed several times with methanol, and the precipitate was dried with a freeze dryer.

Cisplatin loading (Fe_3O_4@SiO_2@ZIF-8@N-Chit-FA-cisplatin)

In order to loading of cisplatin, a ratio of Fe_3O_4@SiO2-ZIF-8@N-Chit-FA (100 ug/mL) and 1 mM aqueous cisplatin (10 mg/10 ml) were tested at a time of 48 h according to Mandriota et al.(Mandriota et al. 2019). The Fe_3O_4@SiO_2-ZIF-8@N-Chit-FA-cisplatin complexes were resuspended in 0.1 M of PBS buffer at pH 7 for stabilization, stirring at approximately 1000 rpm at room temperature. The magnetic nanocarrier was washed three times with external magnets and then resuspended in ultrapure water to remove the remaining cisplatin. The following equation is used to determine the loading efficiency of the drug:

$$\text{Encapsulation efficiency (\%)} = (C_{en} - C_{in}) \times 100$$

In which C_{en} and C_{in} represent the amount of encapsulated cisplatin over its input quantity during the process (mg).

Cisplatin release from Fe_3O_4@SiO_2@ZIF-8@N-Chit-FA

Cisplatin release from Fe_3O_4@SiO_2-ZIF-8@N-Chit-FA nanocarriers at 37 °C during a 4-h-period under different pH conditions for various amounts of time was measured, then centrifuged to calculate the amount of released cisplatin (Günday et al. 2020; Vandghanooni et al. 2020). Using an absorbance at 290 nm, the amount of released cisplatin was calculated. In order to calculate the drug release ratio for cisplatin, the following equation has been used:

$$\text{Adsorption (\%)} = C_0 - C_1/C_0 \times 100$$

In which C_0 and C_1 correspond to the initial concentration of cisplatin (mg) – free cisplatin concentration (mg).

In vivo intraperitoneal administration under an external magnetic field

Fe_3O_4 @ SiO_2-ZIF-8 @ N-Chit-FA-cisplatin was tested on TC1 tumor models to explore its anticancer properties. C57BL/6 mice (20−30 g) were purchased from the Laboratory Animal Center of Mashhad University of Medical Sciences (MUMS), Mashhad, Iran. An Ethical Committee at the Experimental Animal Center of MUMS, Mashhad, Iran, approved all protocols for animal experimentation. During the experiments, the mice were housed in a laboratory environment (with 12 h of light and 12 h of darkness), and standard food and water were provided. The mice were injected subcutaneously with cell suspensions (1×10^6/100 µL) of TC1 cells suspended in RPMI-1640 medium and approximately two weeks later; when the tumors reached a size of 80–100 mm^3(Ghaemi et al. 2012), they were divided into three groups randomly as follows ($n = 6$ in each group): I. Control (Untreated group), II. Cisplatin (treated with 5 mg/kg twice at a 3-day interval, intraperitoneal; IP), and III. Fe_3O_4 @ SiO_2- ZIF-8 @ N-Chit- FA-cisplatin (treated with 5 mg / kg twice at a 3-day interval, IP), after which a circular external magnet (10 mm by 10 mm, surface field strength 0.4 T) was fixed over the tumor area. Tumor measurements were conducted every other day on the animals. The tumor volume (V) was calculated according to the formula V = AB2/2, where A is the length of the major axis and B is the length of the minor axis. To calculate the tumor volume (V), we used the following formula V = AB2/2 (A = the major axis length and B = the minor axis length (Asgharzadeh et al. 2022). A cervical tumor was collected from each mouse on day 18 for further investigation by hematoxylin and eosin (H&E) staining methods.

Characterizations

We characterized the materials using UV–Vis spectrometers (Perkin Elmer Lambda 25) to measure absorbance from 200 to 800 nm.20,26 FT-IR spectra in the 400–4000 cm^{-1} range were obtained using a JASCO FT-IR-460 spectrometer. Structured nanocomposites were characterized by field emission scanning electron microscopy (FESEM) (FESEM, TESCAN MIRA-3) operating at 17 kV and transmission electron

microscopy (TEM) using a JEOL at 300 kV (JEM2100F) for analyzing the morphology and size of synthesized nanomaterials. Powder X-ray diffraction (XRD) spectra were collected using Cu Ka radiation at 1.54056 A wavelength using a Philips PW1730 diffractometer. The magnetic properties of magnetic nanocomposites were determined by vibrating sample magnetometers (Kashan University, Kashan, Iran).

Results and discussion

Figure 2(a–d) depicts the XRD patterns of Fe_3O_4@SiO2, Fe_3O_4@SiO_2-ZIF-8, Fe_3O_4@SiO_2-ZIF-8@N-Chit-FA, and Fe_3O_4@SiO_2-ZIF-8@N-Chit-FA-cisplatin. The cisplatin loading over the Fe_3O_4@SiO_2-ZIF-8@N-Chit-FA nanocomposite was carried out using an enforced adsorption technique. A characteristic sharp peak was observed between 15 and 30 degrees due to the Metal–organic framework ZIF-8. The Fe_3O_4 presence was expected to be observed at 2 theta value of 35.7° in all the nanocomposite structures. The presence of weak XRD peaks was observed corresponding to the core–shell structure of Fe_3O_4 (Fig. 2a, b). Such weak peaks are due to the presence of small nanosized Fe_3O_4, which indicates that nanoporous space was not crystallized inside cages of nanocarriers. The metal–organic framework ZIF-8 has a cage-like structure with many pores, depicting the broad peak in the spectra. However, still, the peak intensities at 35.5°, 43.3°, 53.5°, and 62.8° increased over Fe_3O_4-SiO_2 corresponding to (310), (400), (422), and (440) °, respectively (Fig. 2c). Fe_3O_4 particles tend to have different surface modifications depending on the structure of the silica and MOF structure. Diffraction patterns of the Pt complex were observed in cisplatin (Fig. 2d). A broad diffraction peak was associated with Fe_3O_4@SiO_2-ZIF-8@N-Chit-FA-cisplatin, indicating MOF and silica in the amorphous phase. There are no cisplatin peaks in the diffraction patterns, indicating a transformation of cisplatin due to confinement in the cubic pores of silica and MOF, enhancing cisplatin solubility.

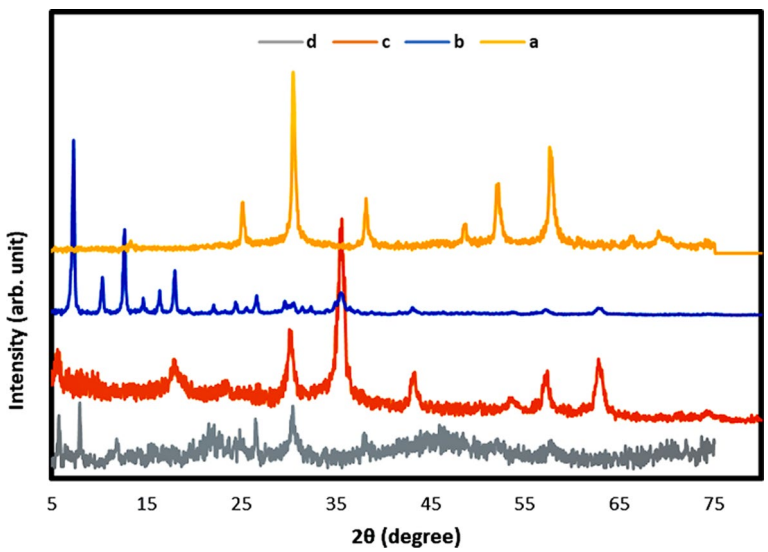

Fig. 2 XRD analysis of **a** Fe_3O_4@SiO_2, **b** Fe_3O_4@SiO_2-ZIF-8, **c** Fe_3O_4@SiO_2-ZIF-8@N-Chit-FA, and **d** Fe_3O_4@SiO_2-ZIF-8@N-Chit-FA-cisplatin

Through FESEM, the surface morphologies of parent and Fe_3O_4@SiO_2-ZIF-8, Fe_3O_4@SiO_2-ZIF-8@N-Chit-FA, and Fe_3O_4@SiO_2-ZIF-8@N-Chit-FA-cisplatin, and cisplatin alone were examined (Fig. 3a–e). The parent Fe_3O_4@SiO_2 was found to be composed of nanosized, spherical spheres of about 27 nm. As a result of the high surface area, iron oxide loaded over SiO_2 did not lead to significant changes in the morphological characteristics compared to the parent material (Fig. 3a). In comparison,

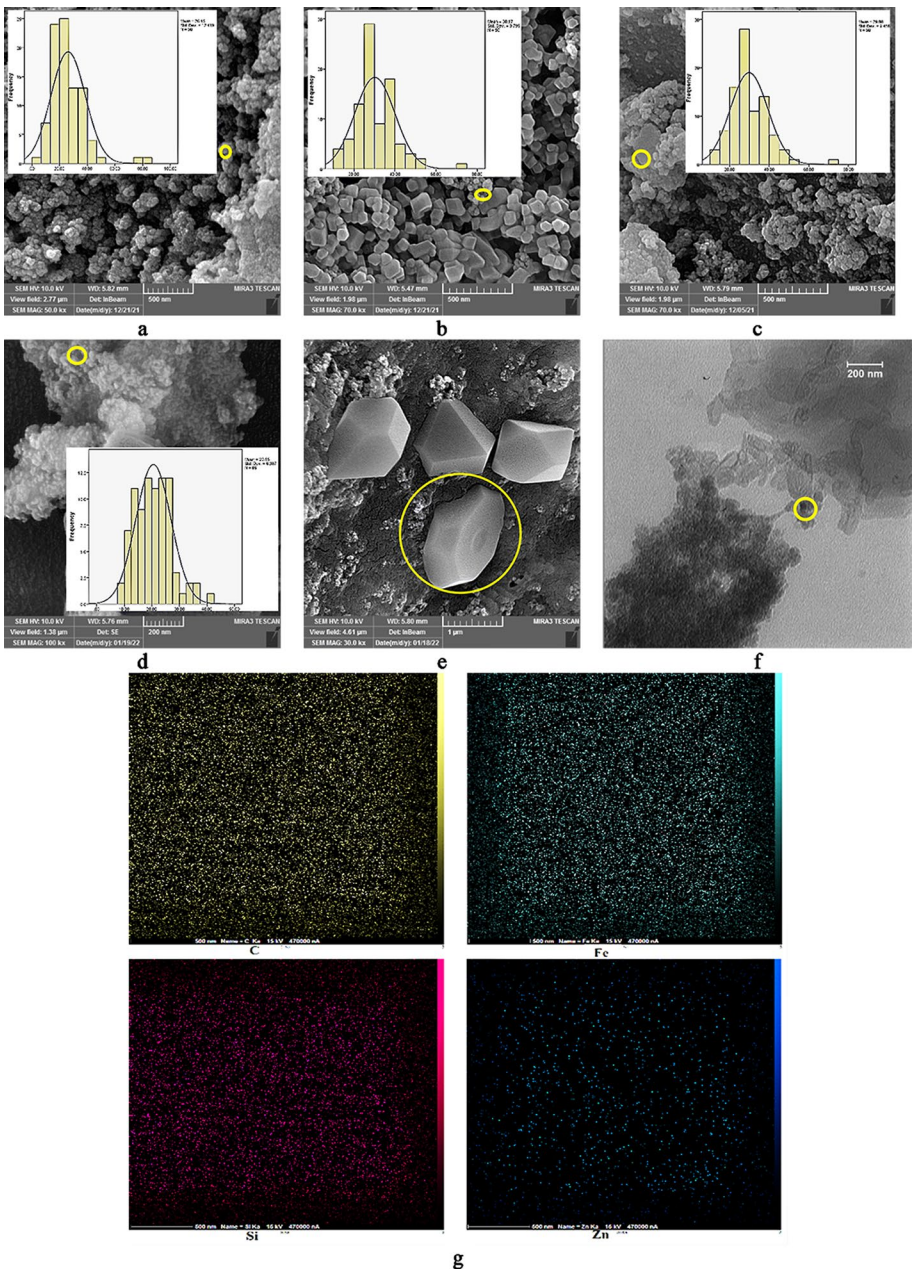

Fig. 3 FESEM analysis of **a** Fe_3O_4@SiO_2, **b** Fe_3O_4@SiO_2-ZIF-8, **c** Fe_3O_4@SiO_2-ZIF-8@N-Chit-FA, and **d** Fe_3O_4@SiO_2-ZIF-8@N-Chit-FA-cisplatin, **e** cisplatin alone (inset: frequencies of particle size and average particle diameter histogram), **f** TEM analysis of Fe_3O_4@SiO_2-ZIF-8@N-Chit-FA, and **g** Map of Fe_3O_4@SiO_2-ZIF-8@N-Chit-FA (C, Fe, Si, and Zn)

the Fe_3O_4@SiO_2-ZIF-8 displayed monodispersed MOF distributed uniformly in the range of about 43 nm. The presence of a hetero nanosized framework over the Fe_3O_4@SiO_2 core–shell was observed for this combination of Fe_3O_4@SiO_2-ZIF-8 (Fig. 3b). In the case of Fe_3O_4@SiO_2-ZIF-8@N-Chit-FA nanocomposite and encapsulated cisplatin on the surface of the nanocomposite, the sample had some porous morphological changes with nanosphere structures at a scale bar of 65, and 55 nm, respectively (Fig. 3c, d). Figure 3f depicts the hexagonal morphology of cisplatin alone used in the *in vivo* studies. Compared with cisplatin alone and nanocomposites, it was demonstrated that cisplatin using *in vivo* studies has shown that nanocomposites have unvarying porous morphology with sizes between 21 and 37 nm, while cisplatin alone has the particle diameter out of nanometer size (around 1500 nm).

According to the TEM analysis at magnifications of 45 nm, Fe_3O_4@SiO_2-ZIF-8@N-Chit-FA nanocomposites have unique deposition characteristics and dependency on the support with the dispersion on the porous core–shell structure of the nanocarriers (Fig. 3f). The particles were grouped based on the particle size: 0–20, 21–30, 31–40, 41–50, 51–60, 61–70, and 71–80 nm. The particle size distribution of Fe_3O_4@SiO_2, Fe_3O_4@SiO_2-ZIF-8, Fe_3O_4@SiO_2-ZIF-8@N-Chit-FA, and Fe_3O_4@SiO_2-ZIF-8@N-Chit-FA-cisplatin was as follows: Fe_3O_4@SiO_2-ZIF-8@N-Chit-FA > Fe_3O_4@SiO_2-ZIF-8@N-Chit-FA-cisplatin > Fe_3O_4@SiO_2-ZIF-8 > Fe_3O_4@SiO_2. From TEM images, a large particle size of about 42.0 ± 1.07 nm was associated with Fe_3O_4@SiO_2-ZIF-8@N-Chit-FA, and SiO_2 shells and ZIF-8 cages support about 18 ± 2.03 nm. From the EDAX mapping analysis, the elemental distribution of the Fe_3O_4@SiO_2-ZIF-8@N-Chit-FA nanocomposite is shown in Fig. 3g. The Fe, Si, Zn, and C atoms were found and are shown in different colors. It was demonstrated that the entire atoms had been distributed in the whole nanocomposite structures uniformity (Fig. 3g). This confirms that a part of the Fe_3O_4@SiO_2-ZIF-8@N-Chit-FA clearly shows the distribution of elements and also an immense perspective to be used in the progress of novel magnetic nanobiocomposite.

Vibrating sample magnetometers (VSMs) were used to measure the magnetic properties of nanoparticle composites. Figure 4(a–d) shows the VSM for the systems, respectively: (a) Fe_3O_4@SiO_2, (b) Fe_3O_4@SiO_2-ZIF-8, (c) Fe_3O_4@SiO_2-ZIF-8@N-Chit-FA, and (d) Fe_3O_4@SiO_2-ZIF-8@N-Chit-FA-cisplatin. The magnetization over three different nanocomposites varied in magnitude. According to Fe_3O_4 magnetization generated over Fe_3O_4@SiO_2, Fe_3O_4@SiO_2-ZIF-8@N-Chit-FA, and Fe_3O_4@SiO_2-ZIF-8@N-Chit-FA-cisplatin nanocomposites, Fe_3O_4@SiO_2 generated the highest value (59.9 $emug^{-1}$), followed by Fe_3O_4@SiO_2-ZIF-8 (40.3 $emug^{-1}$), Fe_3O_4@SiO_2-ZIF-8@N-Chit-FA (36.5 $emug^{-1}$), and Fe_3O_4@SiO_2-ZIF-8@N-Chit-FA-cisplatin (26.3 $emug^{-1}$). Nanoclusters of smaller sizes have been discovered to form superparamagnetic interactions between iron oxide species in core–shell structure SiO_2, while larger nanoclusters contribute to magnetic behavior. An impregnation of Fe_3O_4 into MOF with large pores produces small nanosized Fe_3O_4 nanocomposites, as is shown in the present study. Based on the TEM (Fig. 3d) study, Fe_3O_4@SiO_2 core–shell was 13 nm in size on average over ZIF-8. The VSM spectrum of Fe_3O_4@SiO_2-ZIF-8 showed superparamagnetic behavior with narrow hysteresis in agreement with TEM analysis. A Fe_3O_4@SiO_2-ZIF-8@N-Chit-FA pore produces medium nanoclusters with

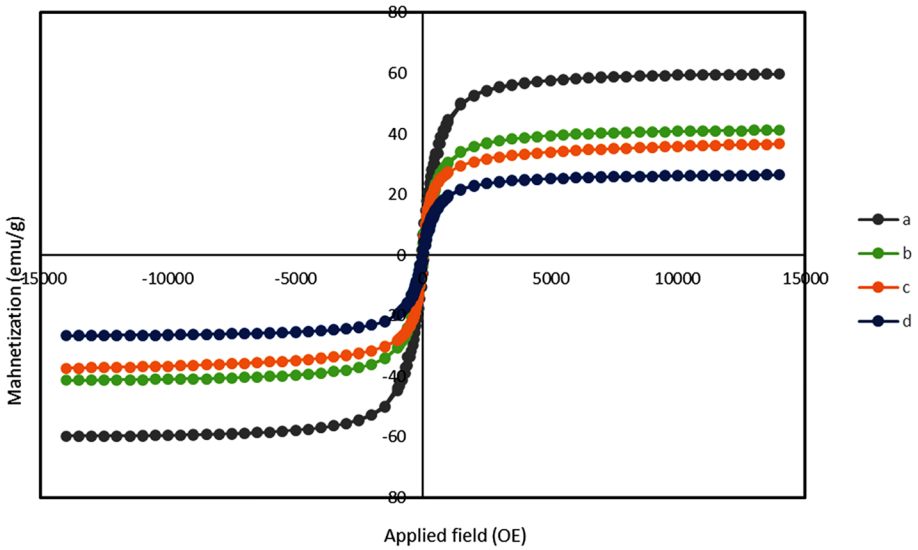

Fig. 4 VSMs analysis of **a** Fe_3O_4@SiO_2, **b** Fe_3O_4@SiO_2-ZIF-8, **c** Fe_3O_4@SiO_2-ZIF-8@N-Chit-FA, and **d** Fe_3O_4@SiO_2-ZIF-8@N-Chit-FA-cisplatin

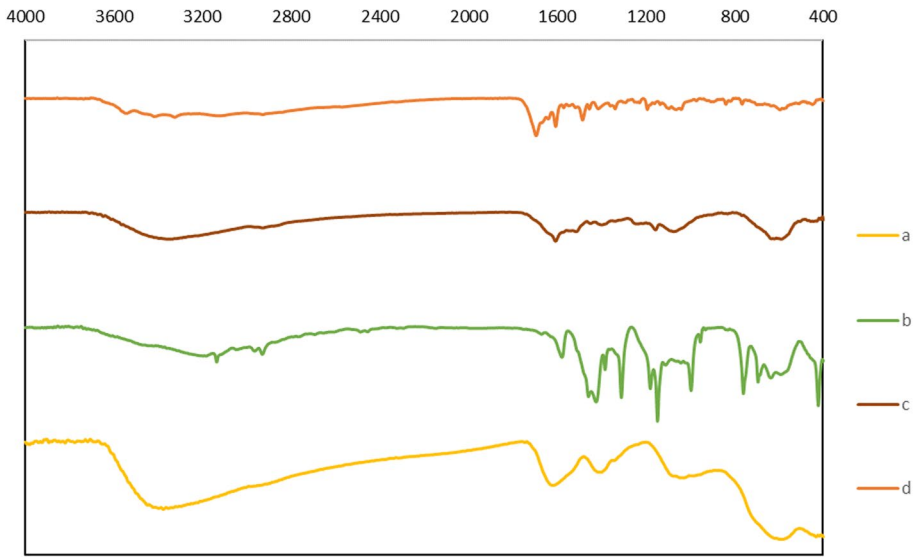

Fig. 5 FT-IR spectra of **a** Fe_3O_4@SiO_2, **b** Fe_3O_4@SiO_2-ZIF-8, **c** Fe_3O_4@SiO_2-ZIF-8@N-Chit-FA, and **d** Fe_3O_4@SiO_2-ZIF-8@N-Chit-FA-cisplatin

an average particle size of 18 nm (Fig. 3e). In contrast to Fe_3O_4@SiO_2-ZIF-8@N-Chit-FA-cisplatin, Fe_3O_4@SiO_2 loaded over monodisperse ZIF-8 produced the strongest magnetization, indicating superparamagnetic behavior.

Following functionalization of magnetic nanoparticle Fe_3O_4 with shells of silane and ZIF-8, FT-IR spectroscopy was used to exhibit interactions and complexes in Fe_3O_4@SiO_2-ZIF-8@N-Chit-FA and Fe_3O_4@SiO_2-ZIF-8@N-Chit-FA-cisplatin (Fig. 5a–d). The spectra analysis of cisplatin revealed strong amine stretching bands at 3338 cm^{-1} and 3267 cm^{-1} and a broad peak at 1654 cm^{-1} as the characteristic peak of cisplatin (Fig. 5). FIT-IR profiles are shown in Fig. 5 for nanocarrier Fe_3O_4@SiO_2, Fe_3O_4@SiO_2-ZIF-8,

Fe_3O_4@SiO_2-ZIF-8@N-Chit-FA, and Fe_3O_4@SiO_2-ZIF-8@N-Chit-FA-cisplatin following iron oxide and silane core–shells. Fe_3O_4@SiO_2-ZIF-8@N-Chit-FA-cisplatin had weak amine bands indicating a conjugated NH_2 of nano-chitosan and OH group of nanocomposite and folic acid toward cisplatin. Furthermore, the bending vibration at 1650 cm^{-1} indicates that cisplatin has been functionalized and the reaction of the folic acid and nano-chitosan and Pt(II) complex was performed.

By utilizing Energy-dispersive, X-ray spectroscopy estimates the percentage of different elements in Fe_3O_4@SiO_2(a), Fe_3O_4@SiO_2-ZIF-8 (b), Fe_3O_4@SiO_2-ZIF-8@N-Chit-FA (c), and Fe_3O_4@SiO_2-ZIF-8@N-Chit-FA-cisplatin (d). The results have shown that FA functionalized chitosan nanocomposite consists of three main organic elements of N, and O with a weight of 12%, and 31%, and main elements of Fi, Si, and Zn with a weight of 10%, 0.5%, and 2% in the core–shell structure. After the encapsulating of drug cisplatin, atomic percentage of O, Fe, Zn, and Si had changed to 27%, 14, 1.30, and 0.5%, respectively. Furthermore, encapsulating of cisplatin on the surface of Fe_3O_4@SiO_2-ZIF-8@N-Chit-FA nanocomposite was demonstrated through 2% element percentage (See Fig. 6).

Antitumor and pro-necrotic effects of magnetic nanobiocomposite in vivo

A murine tumor model was used to determine if Fe_3O_4@SiO_2-ZIF-8@N-Chit-FA-cisplatin inhibits the growth of cervical tumors. The mice were treated with Fe_3O_4@SiO_2-ZIF-8@N-Chit-FA-cisplatin or cisplatin alone, and tumor weight and size were assessed on each group. According to data from experiments, Fe_3O_4@SiO_2-ZIF-8@N-Chit-FA-cisplatin decreased tumor size and weight in mice (Fig. 7 A, B). Fe_3O_4@SiO_2-ZIF-8@N-Chit-FA-cisplatin exerts an enhanced anticancer activity when compared with cisplatin

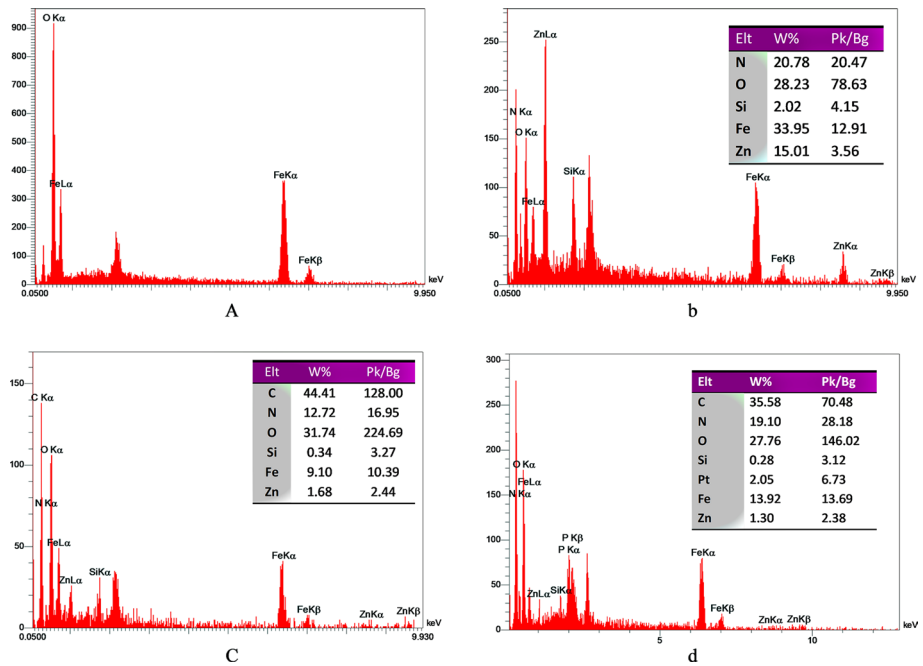

Fig. 6 EDX analysis of particle constituents of **a** Fe_3O_4@SiO_2, **b** Fe_3O_4@SiO_2-ZIF-8, **c** Fe_3O_4@SiO_2-ZIF-8@N-Chit-FA, and **d** Fe_3O_4@SiO_2-ZIF-8@N-Chit-FA-cisplatin

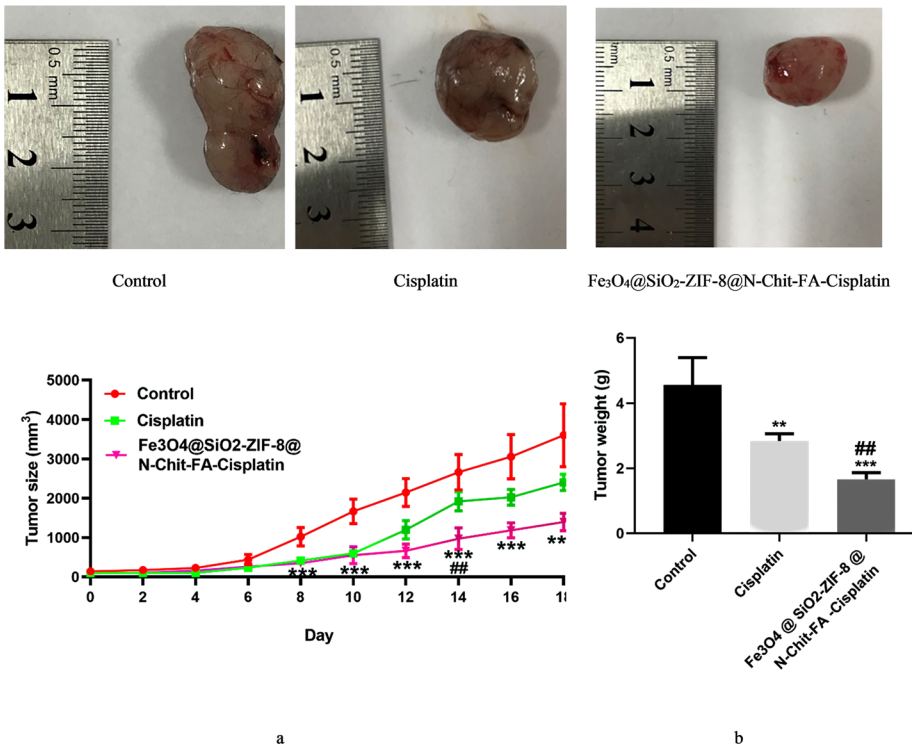

Fig. 7 Fe_3O_4 @SiO_2-ZIF-8 @ N-Chit-FA-cisplatin reducing tumor size and tumor weight in cervical cancer tumor. Effect of Fe_3O_4@SiO_2-ZIF-8 @ N-Chit-FA-cisplatin and cisplatin on tumor size **a** during experiment and tumor weight **b** at the last of experiment in cervical cancer mouse model

alone; consequently, Fe_3O_4@SiO_2-ZIF-8@N-Chit-FA-cisplatin enhanced cisplatin's anti-tumor activities in this cervical cancer model. Cisplatin alone follows a one-compartment model in vivo based on the in vivo release profile of nanobiocomposite. As a result, the magnetic nanobiocomposites are composed of multiple compartments that release in bursts and then release continuously.

A challenge in treating cervical cancer is how to prevent the accumulation of cancer-fighting drugs in healthy tissue while improving the local accumulation of anticancer drugs in the tumor sites (Koning et al. 2010). Nanoparticles with magnetic properties may offer new possibilities for localized cancer treatment (Kumar and Mohammad 2011). A polymeric nanocapsule containing 5-Fu has recently been reported to exhibit similar behavior in the treatment of colon cancer (Li et al. 2008). Shakeri-Zadeh et al. found that 5-Fu had increased colon tumor tissue tendency when loaded into magnetic nanoparticles (Shakeri-Zadeh et al. 2014). In this regard, our in vivo experiments have shown that when carbon nanoparticles are loaded with cisplatin, it has a sustained release, prolonged half-life, and increases tumor tissue uptake.

Figure 8A demonstrates that Fe_3O_4@SiO_2-ZIF-8@N-Chit-FA-cisplatin resulted in an increased area of tissue necrosis in the cervix tumor. A comparison of Fe_3O_4@SiO_2-ZIF-8@N-Chit-FA-cisplatin and cisplatin alone as the standard chemotherapeutic regimen in cervical cancer revealed that Fe_3O_4@SiO_2-ZIF-8@N-Chit-FA-cisplatin increased the percent of necrosis in cervical tissues (Fig. 8, B; p0.05). The necrosis area in H & E-stained section is indicated with arrows.

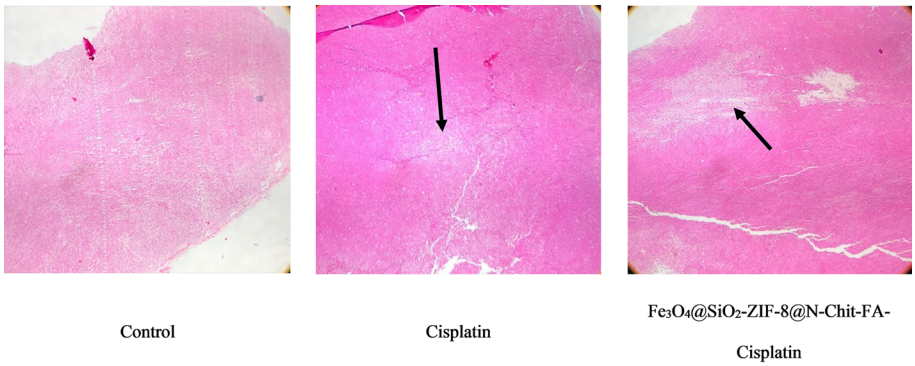

a

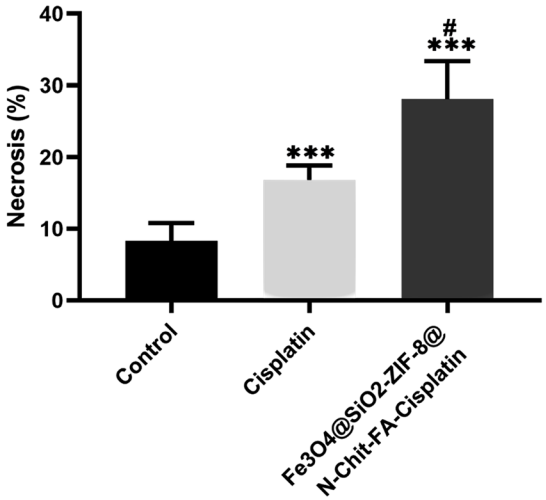

b

Fig. 8 Fe_3O_4 @SiO_2-ZIF-8@ N-Chit-FA-cisplatin promoting necrosis in cervical cancer tumor. Necrosis areas within tumor shown by H&E staining observed with light microscope (**a**). The arrows indicate necrosis area. Quantification of necrotic area with image J software (**b**)

Conclusion

In summary, we have prepared versatile magnetic nanocarrier Fe_3O_4@SiO_2-ZIF-8@N-Chit-FA, further modifying the structure with targeting ligands has led to promote the targeted delivery of cisplatin to cancerous cells in the biological media. The functionalized and magnetic Fe_3O_4@SiO_2-ZIF-8@N-Chit-FA nanocarrier with average diameter 42.0 ± 1.07 nm exhibited high release pores with large windows. By using external magnetic fields in chemotherapy, Fe_3O_4@SiO_2-ZIF-8@N-Chit-FA nanocomposites were able to prevent drug leakage and enhance cancer treatment efficacy in tumor-bearing mice. Additionally, the magnetic nanocomposite demonstrated excellent antitumor activity against cervical cancer isografts. It may be possible to significantly reduce the adverse effects of cisplatin therapy by delivering it with magnetic nanocomposite and to improve the therapeutic index of cisplatin through our method of delivering cisplatin loaded with magnetic nanocomposite. Overall, using Fe_3O_4@SiO_2-ZIF-8@N-Chit-FA not only

expands the applications of functionalized magnetic MOF nanocomposites but also offers new opportunities for developing effective and safe targeted therapeutic carriers that may help gain insight into cancer treatment.

Acknowledgements
The authors gratefully acknowledge the Mashhad University of Medical Science.

Author contributions
MD contributed to visualization, investigation, formal analysis, analysis of data, writing original draft, and methodology. SEN contributed to conceptualization, methodology, visualization, investigation, and formal analysis. FA was involved in analysis of data, methodology, investigation, and writing—original draft. NK-T and TD were involved in methodology and visualization. GK-T and MM contributed to methodology. MK contributed to methodology and writing—review & editing. GAF and AA were involved in writing—review & editing. MR contributed to supervision, funding acquisition, conceptualization, and writing-–review and editing. MK was involved in supervision, funding acquisition, conceptualization, writing-–review and editing, and validation. All authors read and approved the final manuscript.

Funding
There is no government funding for this paper.

Availability of data and materials
All the data sharing not applicable to this article as no dataset was generated or analyzed during the current study. This manuscript contains all the required data to support the findings of this study.

Declarations

Ethics approval and consent to participate
It was not applicable.

Consent of publication
All the authors contributed to the article and approved the submitted version.

Competing interests
The authors declare no competing interests.

Author details
[1]Metabolic Syndrome Research center, Department of Physiology, Faculty of Medicine, Mashhad University of Medical Science, Mashhad, Iran. [2]Department of Medical Biotechnology and Nanotechnology, School of Science, Mashhad University of Medical Science, Mashhad, Iran. [3]Medical Genetic Research Centre, Mashhad University of Medical Science, Mashhad, Iran. [4]Metabolic Syndrome Research Centre, Mashhad University of Medical Science, Mashhad, Iran. [5]Department of Microbiology and Virology, Faculty of Medicine, Mashhad University of Medical Sciences, Mashhad, Iran. [6]Brighton & Sussex Medical School, Division of Medical Education, Falmer, Brighton, Sussex, UK. [7]Medical Toxicology Research Centre, Mashhad University of Medical Science, Mashhad, Iran.

Received: 16 July 2022 Accepted: 10 October 2022
Published online: 02 November 2022

References

Abedi M, Abolmaali SS, Abedanzadeh M, Borandeh S, Samani SM, Tamaddon AM (2019) Citric acid functionalized silane coupling versus post-grafting strategy for dual pH and saline responsive delivery of cisplatin by Fe3O4/carboxyl functionalized mesoporous SiO2 hybrid nanoparticles: a-synthesis, physicochemical and biological characteriz. Mater Sci Eng C 104:109922

Adiga D, Eswaran S, Pandey D, Sharan K, Kabekkodu SP (2021) Molecular landscape of recurrent cervical cancer. Crit Rev Oncol Hematol 157:103178

Alishahi A, Mirvaghefi A, Tehrani MR, Farahmand H, Koshio S, Dorkoosh FA et al (2011) Chitosan nanoparticle to carry vitamin C through the gastrointestinal tract and induce the non-specific immunity system of rainbow trout (Oncorhynchus mykiss). Carbohydr Polym 86(1):142–6

Arbyn M, Weiderpass E, Bruni L, de Sanjosé S, Saraiya M, Ferlay J et al (2020) Estimates of incidence and mortality of cervical cancer in 2018: a worldwide analysis. Lancet Glob Heal 8(2):191–203

Asgharzadeh F, Mostafapour A, Ebrahimi S, Amerizadeh F, Sabbaghzadeh R, Hassanian SM et al (2022) Inhibition of angiotensin pathway via valsartan reduces tumor growth in models of colorectal cancer. Toxicol Appl Pharmacol 440:115951

Azizi S, Darroudi M, Soleymani J, Shadjou N (2021) Tb2(WO4)3@N-GQDs-FA as an efficient nanocatalyst for the efficient synthesis of β-aminoalcohols in aqueous solution. J Mol Liq 329:115555

Boyer C, Whittaker MR, Bulmus V, Liu J, Davis TP (2010) The design and utility of polymer-stabilized iron-oxide nanoparticles for nanomedicine applications. NPG Asia Mater 2(1):23–30

Cheng K, Yang XQ, Zhang XS, Chen J, An J, Song YY et al (2018) High-security nanocluster for switching photodynamic combining photothermal and acid-induced drug compliance therapy guided by multimodal active-targeting imaging. Adv Funct Mater. 28(36):1803118. https://doi.org/10.1002/adfm.201803118

Chon HS, Marchion DC, Xiong Y, Chen N, Bicaku E, Stickles XB et al (2012) The BCL2 antagonist of cell death pathway influences endometrial cancer cell sensitivity to cisplatin. Gynecol Oncol 124(1):119–24
Darroudi M, Ranjbar S, Esfandiar M, Khoshneviszadeh MM, Hamzehloueian M, Khoshneviszadeh MM et al (2020) Synthesis of novel triazole incorporated thiazolone motifs having promising antityrosinase activity through green nanocatalyst CuI-Fe 3 O 4 @SiO 2 (TMS-EDTA). Appl Organomet Chem 34(12):e5962. https://doi.org/10.1002/aoc.5962
Darroudi M, Gholami M, Rezayi M, Khazaei M (2021) An overview and bibliometric analysis on the colorectal cancer therapy by magnetic functionalized nanoparticles for the responsive and targeted drug delivery. J Nanobiotechnol. https://doi.org/10.1186/s12951-021-01150-6
FarahnakRoudsari S, RajabiIslami H, Mousavi SA, Shamsaie MM (2021) Folic acid-coated nanochitosan ameliorated the growth performance, hematological parameters, antioxidant status, and immune responses of rainbow trout (Oncorhynchus mykiss). Front Vet Sci 8:527
Ghaemi A, Soleimanjahi H, Razeghi S, Gorji A, Tabaraei A, Moradi A et al (2012) Genistein induces a protective immunomodulatory effect in a mouse model of cervical cancer. Iran J Immunol 9(2):119–27
Ghasemi K, Darroudi M, Rahimi M, Rouh H, Gupta AR, Cheng C et al (2021) Magnetic AgNPs/Fe3O4@chitosan/PVA nanocatalyst for fast one-pot green synthesis of propargylamine and triazole derivatives. New J Chem 45(35):16119–30
Gonciar D, Mocan T, Matea CT, Zdrehus C, Mosteanu O, Mocan L et al (2019) Nanotechnology in metastatic cancer treatment: current achievements and future research trends. J Cancer. https://doi.org/10.7150/jca.28394
Günday C, Anand S, Gencer HB, Munafò S, Moroni L, Fusco A et al (2020) Ciprofloxacin-loaded polymeric nanoparticles incorporated electrospun fibers for drug delivery in tissue engineering applications. Drug Deliv Transl Res 10(3):706–20. https://doi.org/10.1007/s13346-020-00736-1
Guo J, Filpponen I, Johansson LS, Mohammadi P, Latikka M, Linder MB et al (2017) Complexes of magnetic nanoparticles with cellulose nanocrystals as regenerable, highly efficient, and selective platform for protein separation. Biomacromolecules 18(3):898–905. https://doi.org/10.1021/acs.biomac.6b01778
He Y, Zheng Z, Liu C, Li W, Zhao L, Nie G et al (2022) Inhibiting DNA methylation alleviates cisplatin-induced hearing loss by decreasing oxidative stress-induced mitochondria-dependent apoptosis via the LRP1–PI3K/AKT pathway. Acta Pharm Sin B 12(3):1305–21
Huang J, Li Y, Orza A, Lu Q, Guo P, Wang L et al (2016) Magnetic nanoparticle facilitated drug delivery for cancer therapy with targeted and image-guided approaches. Adv Funct Mater. 26(22):3818–36. https://doi.org/10.1002/adfm.201504185
Jafari Z, Bigham A, Sadeghi S, Dehdashti SM, Rabiee N, Abedivash A et al (2022) Nanotechnology-abetted astaxanthin formulations in multimodel therapeutic and biomedical applications. J Med Chem 65(1):2–36. https://doi.org/10.1021/acs.jmedchem.1c01144
Jermy BR, Alomari M, Ravinayagam V, Almofty SA, Akhtar S, Borgio JF et al (2019) SPIONs/3D SiSBA-16 based multifunctional nanoformulation for target specific cisplatin release in colon and cervical cancer cell lines. Sci Rep 9(1):1–12
Jermy BR, Almohazey D, Alamoudi WA, Palanivel RM, AlSudairi N, Dafalla H et al (2021) Synergistic action of curcumin and cisplatin on spinel ferrite/hierarchical MCM-41 nanocomposite against MCF-7, HeLa and HCT 116 cancer cell line. Cancer Nanotechnol 12(1):1–21. https://doi.org/10.1186/s12645-021-00106-7
Kashyap D, Tuli HS, Yerer MB, Sharma A, Sak K, Srivastava S et al (2021) Natural product-based nanoformulations for cancer therapy: opportunities and challenges. Semin Cancer Biol. 69:5–23
Koning GA, Eggermont AMM, Lindner LH, Ten Hagen TLM (2010) Hyperthermia and thermosensitive liposomes for improved delivery of chemotherapeutic drugs to solid tumors. Pharm Res. https://doi.org/10.1007/s11095-010-0154-2
Kuang Y, Liu J, Liu Z, Zhuo R (2012) Cholesterol-based anionic long-circulating cisplatin liposomes with reduced renal toxicity. Biomaterials 33(5):1596–606
Kumar CSSR, Mohammad F (2011) Magnetic nanomaterials for hyperthermia-based therapy and controlled drug delivery. Adv Drug Deliv Rev 63:789–808
LaVigne AW, Triedman SA, Randall TC, Trimble EL, Viswanathan AN (2017) Cervical cancer in low and middle income countries: Addressing barriers to radiotherapy delivery. Gynecol Oncol Rep. https://doi.org/10.1016/j.gore.2017.08.004
Lee N, Yoo D, Ling D, Cho MH, Hyeon T, Cheon J (2015) Iron oxide based nanoparticles for multimodal imaging and magnetoresponsive therapy. Chem Rev. https://doi.org/10.1021/acs.chemrev.5b00112
Li S, Wang A, Jiang W, Guan Z (2008) Pharmacokinetic characteristics and anticancer effects of 5-Fluorouracil loaded nanoparticles. BMC Cancer 8(1):1–9. https://doi.org/10.1186/1471-2407-8-103
Luo Y, Wu Y, Huang H, Yi N, Chen Y (2021) Emerging role of BAD and DAD1 as potential targets and biomarkers in cancer. Oncol Lett 22(6):1–13
Lv Y, Ding D, Zhuang Y, Feng Y, Shi J, Zhang H et al (2019) Chromium-Doped Zinc Gallogermanate@Zeolitic Imidazolate Framework-8: A Multifunctional Nanoplatform for Rechargeable in Vivo Persistent Luminescence Imaging and pH-Responsive Drug Release. ACS Appl Mater Interfaces 11(2):1907–16. https://doi.org/10.1021/acsami.8b19172
Maillard M, Le Louedec F, Thomas F, Chatelut E (2020) Diversity of dose-individualization and therapeutic drug monitoring practices of platinum compounds: a review. Expert Opin Drug Metab Toxicol. https://doi.org/10.1080/17425255.2020.1789590
Mandriota G, Di Corato R, Benedetti M, De Castro F, Fanizzi FP, Rinaldi R (2019) Design and application of cisplatin-loaded magnetic nanoparticle clusters for smart chemotherapy. ACS Appl Mater Interfaces 11(2):1864–75. https://doi.org/10.1021/acsami.8b18717
Mitsudomi T, Morita S, Yatabe Y, Negoro S, Okamoto I, Tsurutani J et al (2010) Gefitinib versus cisplatin plus docetaxel in patients with non-small-cell lung cancer harbouring mutations of the epidermal growth factor receptor (WJTOG3405): an open label, randomised phase 3 trial. Lancet Oncol 11(2):121–8
Nejadshafiee V, Naeimi H, Goliaei B, Bigdeli B, Sadighi A, Dehghani S et al (2019) Magnetic bio-metal–organic framework nanocomposites decorated with folic acid conjugated chitosan as a promising biocompatible targeted theranostic system for cancer treatment. Mater. Sci. Eng. C. 99:805–15

Paskeh MDA, Mirzaei S, Gholami MH, Zarrabi A, Zabolian A, Hashemi M et al (2021) Cervical cancer progression is regulated by SOX transcription factors: revealing signaling networks and therapeutic strategies. Biomed Pharmacother. https://doi.org/10.1016/j.biopha.2021.112335
Pecorino L (2021) Molecular biology of cancer mechanisms, targets, and therapeutics. Oxford University Press, Fifth Edit
Qin YT, Peng H, He XW, Li WY, Zhang YK (2019) PH-responsive polymer-stabilized ZIF-8 nanocomposites for fluorescence and magnetic resonance dual-modal imaging-guided chemo-/photodynamic combinational cancer therapy. ACS Appl Mater Interfaces 11(37):34268–81. https://doi.org/10.1021/acsami.9b12641
Rabiee N, Ahmadi S, Fatahi Y, Rabiee M, Bagherzadeh M, Dinarvand R et al (2021) Nanotechnology-assisted microfluidic systems: from bench to bedside. Nanomedicine. https://doi.org/10.2217/nnm-2020-0353
Rahimnejad M, NasrollahiBoroujeni N, Jahangiri S, Rabiee N, Rabiee M, Makvandi P et al (2021) Prevascularized micro-/nano-sized spheroid/bead aggregates for vascular tissue engineering. Nano-Micro Lett 13(1):1–24. https://doi.org/10.1007/s40820-021-00697-1
Rahimnejad M, Rabiee N, Ahmadi S, Jahangiri S, Sajadi SM, Akhavan O et al (2021) Emerging phospholipid nanobiomaterials for biomedical applications to Lab-on-a-Chip, drug delivery, and cellular engineering. ACS Appl Bio Mater. https://doi.org/10.1021/acsabm.1c00932
RamezaniFarani M, Azarian M, Heydari Sheikh Hossein H, Abdolvahabi Z, MohammadiAbgarmi Z, Moradi A et al (2022) Folic acid-adorned curcumin-loaded iron oxide nanoparticles for cervical cancer. ACS Appl Bio Mater 5(3):1305–18. https://doi.org/10.1021/acsabm.1c01311
Ramkumar V, Mukherjea D, Dhukhwa A, Rybak LP (2021) Oxidative stress and inflammation caused by cisplatin ototoxicity. Antioxidants. https://doi.org/10.3390/antiox10121919
Rashid M, Zaid AQ (2018) Trends in nanotechnology for practical applications nanosci nanotechnol drug delivery system. Elsevier, Amsterdam
Rojas S, Arenas-Vivo A, Horcajada P (2019) Metal-organic frameworks: a novel platform for combined advanced therapies. Coord Chem Rev 388:202–26
Shakeri-Zadeh A, Shiran MB, Khoee S, Sharifi AM, Ghaznavi H, Khoei S (2014) A new magnetic nanocapsule containing 5-fluorouracil: In vivo drug release, anti-tumor, and pro-apoptotic effects on CT26 cells allograft model. J Biomater Appl 29(4):548–56. https://doi.org/10.1177/0885328214536940
Siegel RL, Miller KD, Jemal A (2019) Cancer statistics, 2019. CA Cancer J Clin 69(1):7–34. https://doi.org/10.3322/caac.21551
Smith BR, Gambhir SS (2017) Nanomaterials for in Vivo imaging. Chem Rev. https://doi.org/10.1021/acs.chemrev.6b00073
Tan J, Tay J, Hedrick J, Yang YY (2020) Synthetic macromolecules as therapeutics that overcome resistance in cancer and microbial infection Biomaterials. Elsevier, Amsterdam
Ulbrich K, Holá K, Šubr V, Bakandritsos A, Tuček J, Zbořil R (2016) Targeted drug delivery with polymers and magnetic nanoparticles: covalent and noncovalent approaches, release control, and clinical studies. Chem Rev. https://doi.org/10.1021/acs.chemrev.5b00589
Vaezifar S, Razavi S, Golozar MA, Karbasi S, Morshed M, Kamali M (2013) Effects of some parameters on particle size distribution of chitosan nanoparticles prepared by ionic gelation method. J Clust 24(3):891–903. https://doi.org/10.1007/s10876-013-0583-2
Vamvakidis K, Mourdikoudis S, Makridis A, Paulidou E, Angelakeris M, Dendrinou-Samara C (2018) Magnetic hyperthermia efficiency and MRI contrast sensitivity of colloidal soft/hard ferrite nanoclusters. J Colloid Interface Sci 511:101–9
Vamvakidis K, Mourdikoudis S, Makridis A, Paulidou E, Angelakeris M, Dendrinou-Samara C (2018) Increase of magnetic hyperthermia efficiency due to optimal size of particles: theoretical and experimental results. J Colloid Interface Sci 511(9):101–9. https://doi.org/10.1007/s11051-020-04986-5
Vandghanooni S, Eskandani M, Barar J, Omidi Y (2020) Antisense LNA-loaded nanoparticles of star-shaped glucose-core PCL-PEG copolymer for enhanced inhibition of oncomiR-214 and nucleolin-mediated therapy of cisplatin-resistant ovarian cancer cells. Int J Pharm 5(573):118729
Vangijzegem T, Stanicki D, Laurent S (2019) Magnetic iron oxide nanoparticles for drug delivery: applications and characteristics. Expert Opin Drug Deliv. https://doi.org/10.1080/17425247.2019.1554647
Wang HS (2017) Metal–organic frameworks for biosensing and bioimaging applications Coordination Chemistry Reviews. Elsevier, Amsterdam
Yang L, Sun H, Liu Y, Hou W, Yang Y, Cai R et al (2018) Self-assembled aptamer-grafted hyperbranched polymer nanocarrier for targeted and photoresponsive drug delivery. Angew Chemie 130(52):17294–8. https://doi.org/10.1002/ange.201809753
ZadehMehrizi T, ShafieeArdestani M, Haji MollaHoseini M, Khamesipour A, Mosaffa N, Ramezani A (2018) Novel nanosized chitosan-betulinic acid against resistant leishmania major and first clinical observation of such parasite in kidney. Sci Rep 8(1):1–19
Zanganeh S, Hutter G, Spitler R, Lenkov O, Mahmoudi M, Shaw A et al (2016) Iron oxide nanoparticles inhibit tumour growth by inducing pro-inflammatory macrophage polarization in tumour tissues. Nat Nanotechnol 11(11):986–94
Zhao S, Zhang Y, Han Y, Wang J, Yang J (2015) Preparation and characterization of cisplatin magnetic solid lipid nanoparticles (MSLNs): Effects of loading procedures of Fe3O4 nanoparticles. Pharm Res 32(2):482–91. https://doi.org/10.1007/s11095-014-1476-2
Zheng H, Zhang Y, Liu L, Wan W, Guo P, Nyström AM et al (2016) One-pot synthesis of metal-organic frameworks with encapsulated target molecules and their applications for controlled drug delivery. J Am Chem Soc 138(3):962–8. https://doi.org/10.1021/jacs.5b11720
Zou Y, Liu YJ, Yang ZP, Zhang DY, Lu YQ, Zheng M et al (2018) Effective and targeted human orthotopic glioblastoma xenograft therapy via a multifunctional biomimetic nanomedicine. Adv Mater 30(51):1803717. https://doi.org/10.1002/adma.201803717

Publisher's Note